Extension and Experimental Demonstration of Gait Transition Network for a Snake Robot

Xin Shu, Chaoquan Tang, *Member, IEEE*, Gongbo Zhou, *Senior Member, IEEE*, Ping Zhou, Lulu Sun, and Xiaodong Yan

***Abstract*—The gait-based control allows the snake robot to move through different environments. The flexible gait transition motion will effectively improve its application in complex environments. To improve the flexibility of gait-based control, this letter proposes a variety of gait transition motions, which extend the gait transition network for snake robots. Firstly, a cost function is designed to guide the parameter conversion within the parameterized gaits based on the sine wave function. Secondly, we choose the crawler gait as the basis to carry out the transition motion design, including the static transition from crawler to serpenoid gait, and the dynamic transition from crawler to ground helix gait and crawler to cylindrical helix gait. Then, we designed a front-end transition method to realize the front-end deformation control of crawler gait. Finally, we report several experiments to verify the effectiveness of the proposed transition motion.**

***Index Terms*—Biologically-inspired robots, motion control, redundant robots, snake robot.**

I. Introduction

THE bionic snake-like robot is widely used in narrow environments and variable shape environments because of its high flexibility and diversity of motion [1]. Gait-based control is used to overcome the high redundancy and difficult control of snake robots [2], [3]. Among them, the more commonly used ones are: serpentine gait [4] for a basic mathematical model of a series of gait including lateral undulation, arc rolling [5] for flat surface, linear progression [6] for narrow space, sidewinding [7] for small-scale obstacles such as sand, crawler gait [8] for large-scale obstacles such as gravel, and helix rolling [9] for cylinder climbing.

In the further study of gait, researchers focus on the kinematics of gait, discuss the influence of gait control parameters on motion performance, or adjust local morphology to improve trafficability. By modeling the rolling gait, [10] completed the configuration adjustment under the arc rolling gait to improve the obstacle climbing ability. [11] discussed the directional control of the snake robot under the sidewinding gait. [12] realized the smooth steering control method of helix rolling gait in inner pipe climbing by connecting two helical lines. [13] reconstruct the backbone curves allow the robot configuration accurately achieve the desired shapes.

In real application scenarios, the geomorphic features will change continuously, which makes any single gait incompetent. One way to solve this problem is to design the transition motion between gaits. Gait transition is often a concern in the research of multi-legged robots [14], [15], but there is relatively little research on snake robots. Based on the neural oscillation network method [16], a smooth transition gait is generated. The distributed method is used to search the optimal switch-times of each joint of the snake robot [17]. Most of these methods focus on the motion details of joints. For the practical application in a changeable environment, there is a lack of a large framework to guide the motion strategy.

In [18], the author simplified the sidewinding motion model to realize the ground navigation, and the arc-rolling gait is used to capture the cylinder, and the helix rolling gait is used to climb the cylinder. We regard such a small transition framework in this literature as an embryonic form of *gait transition network*. The node means the gait, and the transition motion between gaits forms the edge. However, in this gait transition network, the transitionable relationship between gait has not been defined or established. In [19], the authors proposed the connecting forms method, which defines the transition conditions between gaits. At the same time, the paper also describes a large-scale framework of the transitionable relationship between gaits, in which the application environment and motion types are used as the classification basis of gait. The proposed framework greatly expands the gait transition network.

However, the existing gait transition network is still not flexible enough. For one, with the increase in joint numbers, the straight form should not be used as much as possible to avoid excessive space requirements. For another example, the crawler gait has high obstacle-surmounting ability and can be used as the main global motion gait, but it has few connection paths with other gaits in the network.

Based on the existing gait transition network, this letter aims to improve the flexibility of gait transition, design gait transition motion in various scenarios, increase the number of transition paths, and extend the gait transition network. The main contributions of this letter are as follows:

1) A variety of transition motions are proposed, and the derivative gaits of crawler gait are designed, including R-crawler, H-crawler and front-end deformed. These extend

Manuscript received 19 July 2022; accepted 17 November 2022. Date of publication 1 December 2022; date of current version 8 December 2022. This letter was recommended for publication by Associate Editor P. Di Lillo and Editor C. Gosselin upon evaluation of the reviewers' comments. This work was supported in part by the National Natural Science Foundation of China under Grants 62233011, 62073328, 61971423, and 61903341, in part by the Fundamental Research Funds for the Central Universities under Grant 2021YCPY0203, and in part by the Project Funded of the Priority Academic Program Development of Jiangsu Higher Education Institutions (PAPD). *(Corresponding authors: Chaoquan Tang; Gongbo Zhou.)*

The authors are with the Jiangsu Key Laboratory of Mine Mechanical and Electrical Equipment, School of Mechatronic Engineering, China University of Mining and Technology, Xuzhou, Jiangsu 221116, China (e-mail: shuxin@cumt.edu.cn; tangchaoquan@cumt.edu.cn; gbzhou@cumt.edu.cn; zhoup@cumt.edu.cn; ts20050051a31@cumt.edu.cn; yanxiaodong@cumt.edu.cn).

Digital Object Identifier 10.1109/LRA.2022.3226066

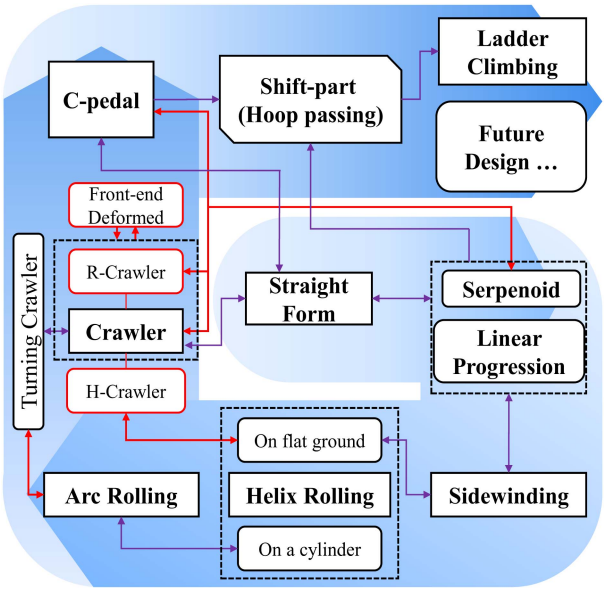

Fig. 1. Gait transition network for snake robot. The blue arrow in the background is the development process of snake robot gait, the purple arrow is the conversion path in the existing literature, and the *red mark* is the work to be carried out in this letter.

the available configurations and improved the connectivity of the gait transition network.

2) The parameter-matching relationship of the transition motion we designed is studied, and all the transition motions are verified by experiments.

II. Problem Statement and Related Work

A. Overview of Gait Transition Network

The gait transition network extended in this letter is constructed on the basis of the transitionable relationship in [19]. In the existing gait transition network, multiple gaits needs to be connected with the straight form, while it needs larger execution space when the number of joints is large, which is not conducive to the flexible use of gaits. On the other hand, some high-performance gait, such as caterpillar gait, have almost no connection with other configurations.

In order to solve the above problems, this letter aims to improve the connectivity of gait transition network, design more convertible configurations, and design transition motion for these configurations.

The red mark in Fig. 1 is the research goal of this letter. The completion of these contents can greatly improve the flexibility of the motion strategy of snake robots in complex environments.

B. Parameterized Gait Control

In a large number of researches on the gait control of snake robots, the initial generation of gait is usually carried out through the expression (1) of the curvature length integral, which is more conducive to the expression of the macro shape of the robot.

$$\theta_i^d = \begin{cases} \int_{s_h+(i-1)l}^{s_h+(i+1)l} \kappa_p(s)\,\mathrm{d}s & (i:\text{odd}) \\ \int_{s_h+(i-1)l}^{s_h+(i+1)l} \kappa_y(s)\,\mathrm{d}s & (i:\text{even}) \end{cases} \tag{1}$$

TABLE I
Parameters of Segments for the Basic Form of the Crawler Gait

seg No. j	shape	parameters	$\hat{\psi}_j$
$3n+1$	SL	$(\kappa,\tau,l)=(0,0,d_C+2R_C)$	0
$3n+2$	Arc	$(\kappa,\tau,l)=(1/R_C,0,\pi R_C)$	$(-1)^n\alpha_C$
$3n+3$	Arc	$(\kappa,\tau,l)=(1/R_C,0,\pi R_C)$	0

(SL is the abbreviation of straight-line, the same below).

$$\psi(s) = \int_0^s \tau(\hat{s})\,\mathrm{d}\hat{s} + \psi(0)$$
$$\kappa_p = -\kappa(s)\sin\psi(s),\ \kappa_y = \kappa(s)\cos\psi(s). \tag{2}$$

For the angle control of each joint motor, the expression (3) based on sinewave is more conducive to the intuitive understanding of each joint angle and its variation characteristics. In this letter, we use (3) to summarize the parameterized gait, and use three key parameters (A, φ, e) to graphically characterize the distribution of the current commonly used parameterized gait, as shown in Fig. 2.

$$\theta(i,t) = \begin{cases} \beta_{\text{odd}} + A_{\text{odd}}\sin(\theta_{\text{odd}}) & (i:\text{odd}) \\ \beta_{\text{even}} + eA_{\text{even}}\sin(\theta_{\text{even}}+\delta) & (i:\text{even}) \end{cases} \tag{3}$$

$$\theta_{\text{odd,even}} = \varphi_{\text{odd,even}} n + w_{\text{odd,even}} t \tag{4}$$

In Fig. 2, the orange plane is a virtual pedestal, which is obtained through the Virtual Chassis method [20]. In this method, SVD method is used to standardize the attitude and orientation of the snake robot.

C. Crawler Gait and its Derivative Configuration

The connecting curve method is proposed in [8], which connects simple characteristic curves by setting a virtual rolling angle. The joint control is to modify $\psi(s)$ in (2) to (5) based on the curvature length integral equation. With the help of connecting curve method, the crawler gait is designed, as shown in Fig. 3(a), and its control parameters are shown in Table I. The joint angle can be obtained by substituting the parameters into (1), (2) and (5).

$$\psi(s) = \int_0^s \tau(\hat{s})\,\mathrm{d}\hat{s} + \psi(0) + \sum_j \hat{\psi}_j u(s-s_j)$$
$$u(s) = \begin{cases} 0, & s<0 \\ 1, & s\geq 0 \end{cases} \tag{5}$$

Three key parameters (R, d, α) of the gait control are extracted to graphically characterize the configuration, as shown in Fig. 3(b). Furthermore, we introduce two derived configurations of crawler gait. The first one is *R-Crawler*, as shown in Fig. 4(a), which is obtained by reversing the rolling angle of curve segment connecting. The second is *H-Crawler*, as shown in Fig. 4(b), which is obtained by replacing the original arc segments with a helix segment. The corresponding control parameters are shown in Tables II and III.

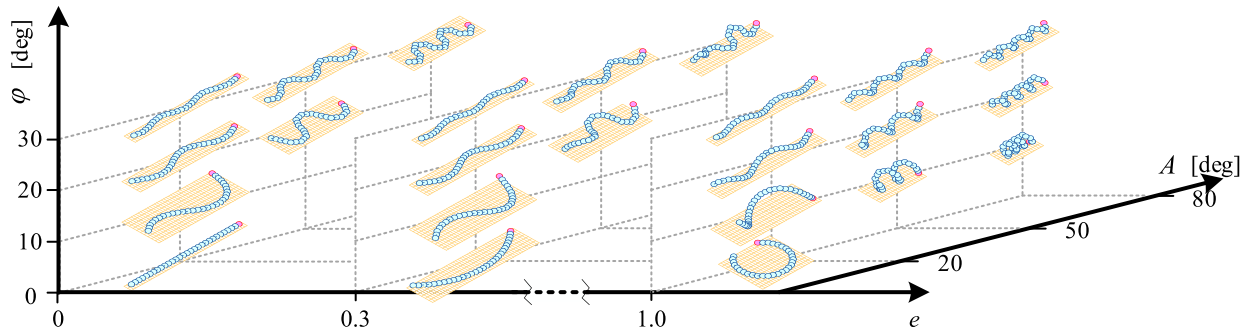

Fig. 2. Parametric distribution of gait configuration changes in sinewave series gaits. The gait joints are controlled by (3). Let $\beta = 0$ as the default, and the corresponding gait parameters are as follows: $A \neq 0, \varphi \neq 0, e = 0$ for serpenoid gait, $A \neq 0, \varphi \neq 0, 0<e<1$ for sidewiding, $A \neq 0, \varphi = 0, e = 1$ for arc rolling, and $A \neq 0, \varphi \neq 0, e = 1$ for helix rolling.

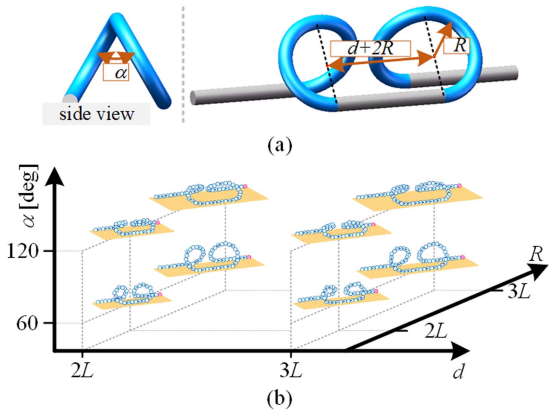

Fig. 3. Basic configuration of crawler gait and its parameter distribution of configuration change. (L means the length of a modular).

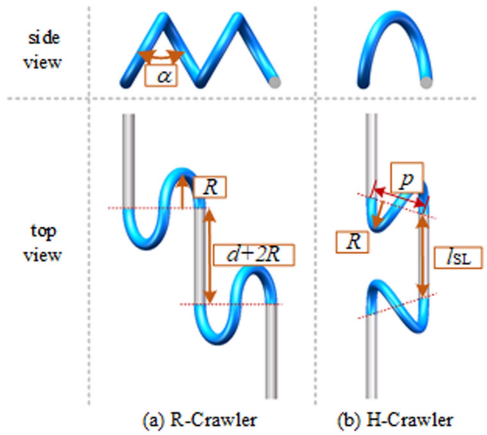

Fig. 4. Derived configurations of crawler gait.

TABLE II
PARAMETERS OF SEGMENTS FOR THE BASIC FORM OF THE R-CRAWLER

seg No. j	shape	parameters	$\hat{\psi}_j$
$3n+1$	SL	$(\kappa,\tau,l)=(0,0,d_C+2R_C)$	0
$3n+2$	Arc	$(\kappa,\tau,l)=(1/R_C,0,\pi R_C)$	α_C
$3n+3$	Arc	$(\kappa,\tau,l)=(1/R_C,0,\pi R_C)$	α_C

TABLE III
PARAMETERS OF SEGMENTS FOR THE BASIC FORM OF THE H-CRAWLER

seg No. j	shape	parameters	$\hat{\psi}_j$
$2n+1$	SL	$(\kappa,\tau,l)=(0,0,l_{SL})$	0
$2n+2$	Helix	$(\kappa,\tau,l)=(R_H/(R_H^2+(\frac{p_H}{2\pi})^2),$ $(-1)^n\frac{p_H}{2\pi}/(R_H^2+(\frac{p_H}{2\pi})^2),$ $2\pi\sqrt{R_H^2+(\frac{p_H}{2\pi})^2})$	0

D. Shape Control and Phase Control of Configuration

When the snake-like robot is controlled by the designed backbone curve, there are usually two ways, shape control and phase control:

1) *Shape control:* refers to changing the integral starting point of the curve, corresponding to s_h in (1), resulting in the change of the configuration shape. Shape control is often used to achieve gait moving along the tangential direction of the backbone, such as crawler gait and stair climbing gait [21].
2) *Phase control:* refers to changing the initial integral phase angle of the curve, corresponding to $\psi(0)$ in (2) & (5). For gaits with odd and even joints having the same periodic characteristics, the intuitive performance is rotation around the body axis. Phase control is often used to achieve gait along the normal direction of the backbone curve, such as the lateral movement of crawler gait. In particular, V-shift control [22] combines two controls to achieve the change of motion mode. On this basis, a series of research on pipeline climbing has been realized [12], [23].

E. Gait Transition at Both Ends of the Backbone

In [19], the author puts forward a general method for connecting forms, which is applicable to both the front and back ends of backbone. Simultaneously, the author also describes the limitations of the front-end connection, but few gait can be applied. For the back-end connection, any tangent backbone can complete the connection theoretically, but some additional restrictions need to be added. In addition to these restrictions, the design of backbone also makes a great difference to the forms connection. Taking the crawler gait as an example, when it is moving, the integral propulsion direction of s_h is opposite

to the motion direction. In response to scene changes, when parameter adjustment or gait transition is required, the integral length s needs to propel a whole robot length to realize the transition, which affects the motion efficiency of the robot. For the front-end connection, hoop-passing is an effective solution, but this method requires that the gait backbone has the ability to form a buffer segment (shift part) to facilitate the tangential propulsion. This letter takes the crawler gait as an example, realizes the parameter adjustment of the front-end backbone when the environment changes, and tries to provide ideas for the front-end gait transition.

III. Methodology

Flexible gait transition motion is an important guarantee for snake robots to efficiently use multi-gait to pass through complex environments. The essence of gait is to control the rotation angle of all joint motors $\boldsymbol{\theta}_n(t)$. The trajectory of $\boldsymbol{\theta}_n(t)$ in n-dimensional space should be an ordered closed curve. Therefore, the process of gait transition can be regarded as the n-dimensional points in joint space jumping from one closed curve to another. It is easy to think of using a straight line to connect the points on two closed curves, and using interpolation to move on the line, so as to achieve gait transition. However, due to a large number of snake robot joints, this method is easy to cause the span of the end trajectory to be too large, which is not conducive to use in the real scene. In order to solve the above problems, the following will discuss the design of gait transition motion in categories.

A. Static Transition

We first consider the case of static transition, which refers to the case where both configuration shape control and phase control are disabled, and the transition process only adjusts the configuration parameters.

1) Transition Motion Based on Control Parameters: In this section, we continue to use the three core parameters in Fig. 2 to describe gait instead of joint space. We first describe the space occupied by the snake robot with the help of the Virtual Chassis method, and then use the space volume difference occupied by the robot before and after gait transition to represent the cost of the transition motion, so as to guide the robot's control parameter conversion.

The backbone of gaits corresponding to a certain range of parameters is calibrated by the Virtual Chassis method, and then the 3D dimension of the chassis is calculated as the 'volume' of the parameter.

$$V_{i\cdot m\cdot n} = (X_{\mathrm{VC}}, Y_{\mathrm{VC}}, Z_{\mathrm{VC}})\,|(A_i, \varphi_m, e_n) \tag{6}$$

Where X_{VC} represents the span in the X direction after the configuration is calibrated by Virtual Chassis. The parameter range is drawn up as $A \in [0, 90]$ deg, $\varphi \in [0, 30]$ deg, $e \in [0, 1]$. Then, calculate the ΔV when the control parameters change as follows, $\pm\Delta A$, $\pm\Delta\varphi$, $\pm\Delta e$.

$$\begin{cases} \Delta V\,|\pm\Delta A = \mathrm{Cost}\left(V_{i\cdot m\cdot n}, V_{(i\pm1)\cdot m\cdot n}\right) \\ \Delta V\,|\pm\Delta\varphi = \mathrm{Cost}\left(V_{i\cdot m\cdot n}, V_{i\cdot(m\pm1)\cdot n}\right) \\ \Delta V\,|\pm\Delta e\ = \mathrm{Cost}\left(V_{i\cdot m\cdot n}, V_{i\cdot m\cdot(n\pm1)}\right) \end{cases} \tag{7}$$

Considering that there are two main resistances to the transition motion, the friction from the ground in the horizontal direction and the gravity in the vertical direction, the dimension changes in different directions of the chassis are simply assigned different weights. The cost function in transition of parameterized gait is defined as follows:

$$\mathrm{Cost}\,(V_1, V_2) = \sqrt{(X_1 - X_2)^2 + (Y_1 - Y_2)^2} + \sigma\,(Z_2 - Z_1) \tag{8}$$

Finally, sum the parameter transition costs in the six directions to represent the cost of the parameter point transferring to the surrounding parameter points, obtain the vector $(A, \varphi, e, \sum \mathrm{Cost})$, and draw the scatter diagram. The results of $\sigma = 1.2$ are shown in Fig. 5.

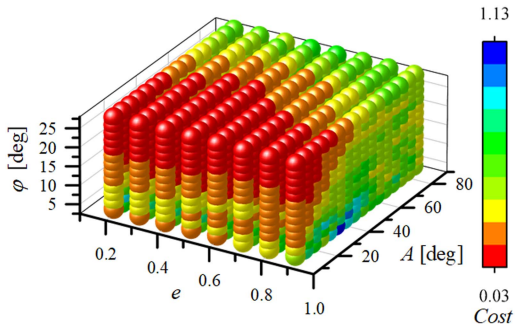

Fig. 5. Transition cost distribution in parameterized gait.

In Fig. 5, the distribution with low transition cost is obvious, mainly in the areas with larger φ and smaller A. For the transition of any two groups of control parameters, in order to reduce the space demand of the process, it should be close to the red area in the figure rather than a straight-line connection.

2) Transition Motion Based on Configuration Matching: Similarly, according to the definition of static transition, this section considers the transition motion only through parameter adjustment and joint linear control. Through the observation of Fig. 2 and Fig. 3, it is considered that only when $\alpha = 0$, the configuration of crawler gait and sinewave gait may have a good similarity. It should be noted that the derived configuration of the crawler gait requires backbone propulsion, which does not meet the requirements of static transition.

The characteristic of serpenoid gait is an S-shaped curve. When $\alpha = 0$, the crawler can be regarded as a straight line segment connecting two arcs. The arc is similar to the S-shape when the curvature is large enough. Combined with such a priori assumption, the transition from crawler gait to serpenoid gait is described as follows:

- The arc length in crawler is equal to the serpenoid S-shaped arc length.

$$R_{\mathrm{C}} \cdot \pi = (\pi/\varphi) \cdot l \tag{9}$$

- The length of the straight line is equal to the length of the arc.

$$2R_{\mathrm{C}} + d = R_{\mathrm{C}} \cdot \pi \tag{10}$$

As shown in Fig. 6, there are mainly two quantities to be controlled in the transition, α and the curvature of the original straight-line segment, $\kappa_{\mathrm{sl}} = \varphi_{\mathrm{sl}}/l_{\mathrm{sl}}$. The gradient of α is to ensure that the robot does not touch the ground too early during the change of curvature κ_{sl}, so as to avoid excessive friction and deformation resistance.

In addition to the basic configuration of crawler, it can also be a transition through R-crawler configuration, gradually changing

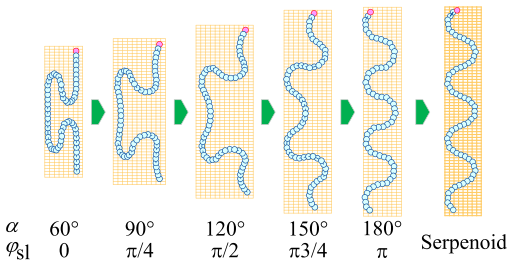

Fig. 6. Static transition from crawler gait to serpenoid gait.

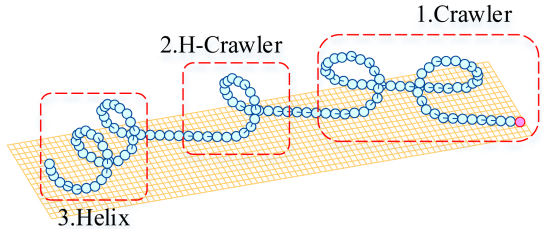

Fig. 7. Dynamic transition from crawler gait to helix gait on the ground.

TABLE IV
SECTIONAL CURVE PARAMETERS OF CONNECTING FORMS OF FIG. 7

Seg No. j	Forms	parameters	$\hat{\psi}_j$
$i+1$	Crawler	(R_C, d_C, α_C)	…
…			
$i+7$			$-\alpha/2$
$i+8$	Helix	$(r_H, p_H) = (R_C \cos\frac{\alpha}{2}, 4R_C \sin\frac{\alpha}{2})$	0
$i+9$	SL	——	0
$i+10$	Helix	$(r_H, p_H) = (R_C \cos\frac{\alpha}{2}, 4R_C \sin\frac{\alpha}{2})$	0

α to 180°, $(d + 2R)$ to 0. Similarly, the C-pedal gait can also use the a similar method, and its process will not be repeated here.

B. Connection at the Back-End of Backbone

In contrast to static transition, dynamic transition completes the transition motion with the help of two control methods. The back-end connection of backbone is the main means to realize gait transition under configuration shape control. Regardless of the direction of movement, with the advance of the initial integration length, the latter joint always repeats the action of the previous joint. When all joints enter the backbone of the next gait, the gait transition is completed.

For the curve connecting any two points in space, in addition to smoothness, the stability of the backbone in the gravity field should also be considered, which leads to the complexity of obtaining the curve equation. Therefore, in the connecting curve method, simple characteristic curves such as straight lines, arcs, and helices are selected as the basic line segments connecting the spatial configuration. It is noted that the virtual roll angle $\psi(\hat{s})$ is used in the method to realize the discretization of torsion, which requires certain prior information for the designed backbone. However, the curvature deflection equations of some commonly used gait backbones are not integrable, which also leads to the failure to obtain the prior information. Therefore, in the next, some appropriate curves will be selected for smooth connection.

1) Constrained Condition: Gait transition by connecting forms is a dynamic process. Only considering the connection of configuration tangents will lead to severe slippage in the transition process, so additional constraints are required. In Section II, we mentioned that the two boundary conditions proposed by [19] serve the hoop-passing motion only. In order to extend the application of connecting forms in gait transition, we modify the boundary conditions and design the transition configuration only considering the ground constraints.

- *Constraint-I:* The movement direction of the connection point in the two frames is consistent.
- *Constraint-II:* The underside of the two frames is coplanar, and the connecting interface is vertical to the backbone lines, which is tangent at the surface.

When the connection point is not at the same height under Constraint-I, it is necessary to add a frame or curve to the two frames for connecting.

2) Configuration Design of Transition Without Phase Control: Helix gait has strict periodic characteristics when applied to cylinder or inner tube climbing. The shape control and phase control of the configuration achieve almost the same effect. However, when it is used in the plane, the difference between the two controls will appear. Shape control makes the configuration roll along the circumference in the form of a wheel. Phase control makes each segment rotate around its own axis, and finally roll along the normal direction of the configuration. In this part, we use the above characteristics of helix gait to design the transition configuration between crawler gait and helix gait.

It is noted that in the derived configurations of crawler gait, the configuration of H-crawler, R-crawler and the original gait meet the two boundary conditions of connecting forms in the straight-line segment. Use above gaits to design the transition configuration, as shown in Fig. 7 and Table IV.

3) Configuration Design of Transition With Phase Control: Flexible use of the two control methods can effectively improve the motion efficiency of the snake robot. However, due to the difference of motion direction between the two controls, most gait can not meet the Constraint-I. In this section, we try to use the change of climbing environment to reduce the impact of the failure of Constraint-I.

Considering that arc rolling can smoothly realize the transition from ground rolling to cylinder climbing, we take the connecting of ground arc rolling to cylinder helix as a part of the transition configuration. It is noted that under the control of phase change, the movement direction of crawler gait can be consistent with that of rolling gait through parameter adjustment. We also take the connecting of crawler to ground arc rolling as another part of the transition configuration. Finally, the transition process from ground crawler to cylindrical helix is shown in Fig. 8, and the curve parameters in Table V.

C. Transition at the Front-End of Backbone

The normal movement of the crawler gait is straight and turning. In this section, we will also consider a case where the channel is suddenly narrowed during the movement, regardless of the height or width direction. Due to the gait control principle, the robot needs to propel an entire length of the robot to move the back-end morphological features to the front-end, which greatly reduces its motion efficiency. One of the ways to solve this problem is to predict the distance through the sensors and design the connecting forms of back-end in advance combined

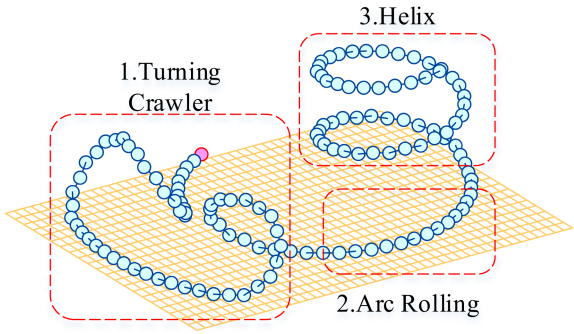

Fig. 8. Dynamic transition from crawler gait to helix gait on a cylinder.

TABLE V
SECTIONAL CURVE PARAMETERS OF CONNECTING FORMS OF FIG. 8

Seg No. j	Forms	parameters	$\hat{\psi}_j$
$i+1$	Turning Crawler	$(R_{\mathrm{C}}, d_{\mathrm{C}}, \alpha_{\mathrm{C}}, R_{\mathrm{Turn}})$	…
…			
$i+7$			0
$i+8$	Arc	$(r_j, \phi_j) = (r_{\mathrm{Arc1}}, \phi_{\mathrm{Arc1}})$	$-\pi/2$
$i+9$	Arc	$(r_j, \phi_j) = (r_{\mathrm{Arc2}}, \mathrm{atan}(p_{\mathrm{H}}/2\pi r_{\mathrm{H}}))$	$\pi/2$
$i+10$	Helix	$(r_j, p_j) = (r_{\mathrm{H}}, p_{\mathrm{H}})$	0

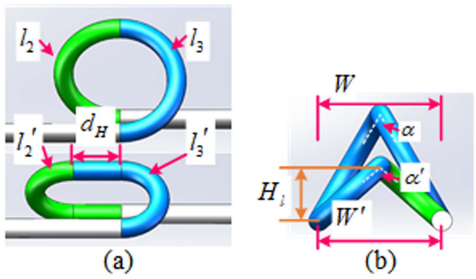

Fig. 9. Configuration limitation of the front segment transition of crawler gait.

with kinematics. However, the sensor system of snake robot is not yet mature, and this kind of motion logic is not conducive to use in the continuously changing environment.

To solve this problem, we propose to modify the shape of front-end of the backbone to deal with the real-time change of the channel size in front of the movement. The following describes the limitations of its deformation and specific implementation methods.

1) Limitations: The friction between the robot and the ground depends on the size of the contact surface and the direction of motion. When the backbone is deformed, the friction can be divided into tangential and normal directions along the backbone. In order to maintain the stability of the configuration, the sliding friction should be avoided as much as possible during the deformation.

The friction in the two directions is analyzed respectively.

- *Tangential sliding:* The straight-line segment should be controlled to be static during deformation, which required the circumference of the lifting segment to remain unchanged. As shown in Fig. 9(a).

$$l_2 + l_3 = l_2' + l_3' \tag{11}$$

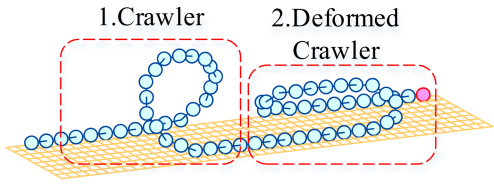

Fig. 10. The deformed configuration of crawler gait.

- *Normal sliding:* The spacing between the two straight line segments should be controlled unchanged during the deformation. As shown in Fig. 9(b).

$$W = W' \tag{12}$$

In this section, the straight motion of gait is mainly studied. It is considered that the friction of deformation along the tangent direction is greater, so when the two conditions cannot be met at the same time, the tangential sliding limitation will be satisfied first.

2) Specific Implementation: According to the limitations and the setting of the environment, the target configuration we designed is shown in Fig. 10. The arc segment is deformed into a combination of straight and arc to reduce the longitudinal space size under the limitation (11), (12). Set the height of the target channel as H_l, and the corresponding constraint conditions are (13). The connection position between the deformed arc segment and the straight-line segment is also adjustable. Moreover, the deformed parallel straight-line segment has a certain degree of coincidence, which also makes the original configuration more stable.

$$\begin{cases} \alpha'/2 = \mathrm{argtan}\left(2R \cdot \sin\left(\alpha/2\right)/H_l - 2r\right) \\ 2R' = \left(H_l - 2r\right)/\cos\left(\alpha'/2\right) \\ d_H = \pi\left(R - R'\right) \end{cases} \tag{13}$$

In practice, we can use (14) as the curve equation of the lifting segment, which can reduce the division of additional integral segments. Moreover, due to the limited number of robot joints in the lifting segment, the shape formed by (14) is almost the same as that of (13), and the corresponding dimension parameters are also universal.

$$\kappa\left(s\right) = \kappa\left(1 + e \cdot \sin\left(2\kappa s - \pi/2\right)\right) \tag{14}$$

In (14), $\kappa = 1/R$, $e \in [0, 1]$. The higher the e value, the more the longitudinal dimension of crawler configuration decreases.

IV. EXPERIMENTAL RESULTS

To verify the proposed gait transition motion for various situations, we use an orthogonal joint snake-like robot for experiments. The product motor (Dynamixel XH540-W270R, ROBOTIS, Ins.) is selected as the driving joint of the robot. Each module is assembled with a shell made of 3D printing of nylon material. In order to expand the allowable angle range between the joints, the length of each module is relatively large. Fig. 11 shows the robot prototype used in the experiment. The length of each module is $l = 96$ mm, the outer diameter of the skin is $d = 68$ mm, the mass of each module is about 214 g, and the number of joints is 30.

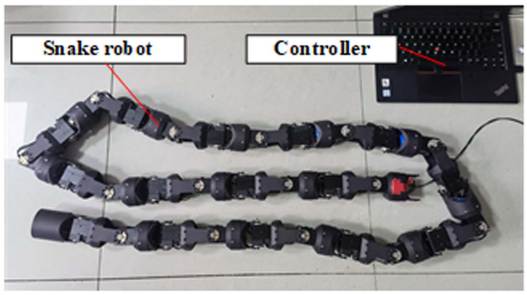

Fig. 11. Snake robot prototype.

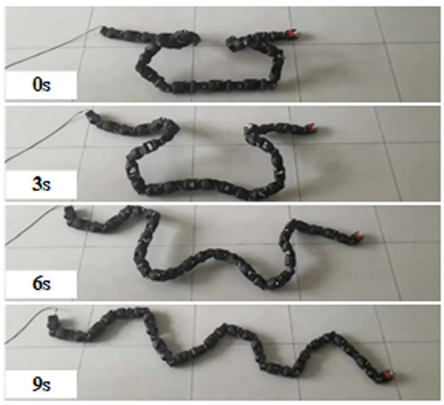

Fig. 12. The transition experiment from crawler gait to serpenoid gait.

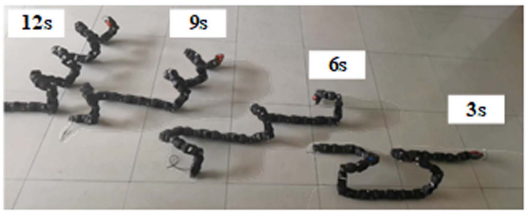

Fig. 13. The transition experiment from crawler gait to helix gait on the ground.

A. Crawler to Serpenoid

The track gait is mainly realized by shape control, and the configuration at different times is quite different. For the convenience of observation, the symmetrical configuration is selected as the initial configuration. Combined with the size of the robot, the parameters of the original crawler are set as $R_{\mathrm{C}} = 140\,\mathrm{mm}, d_{\mathrm{C}} = R_{\mathrm{C}}(\pi - 2)$. According to the constraints of (9), (10), the parameters of the target serpenoid gait are set as $\varphi = l/R_{\mathrm{C}}$. The experimental results are shown in Fig. 12.

B. Crawler to Helix

The realization of crawler gait to helix rolling gait is mainly affected by ground constraints and motion direction constraints. The parameters of each segment are set on the basis of $R_{\mathrm{C}} = 130\,\mathrm{mm}, d_{\mathrm{C}} = 160\,\mathrm{mm}, \alpha_{\mathrm{C}} = 70^{\circ}$. In the process, $r_{\mathrm{H}} = R_{\mathrm{C}}\cos(\alpha_{\mathrm{C}}/2)$ and $p_{\mathrm{H}} = 4R_{\mathrm{C}}\sin(\alpha_{\mathrm{C}}/2)$ are controlled so that the spatial scale of the configuration does not change. The experimental results are shown in Fig. 13. It can be seen from the experiment, that the gait transition motion by the connecting forms is very smooth, and the configuration is also very stable under constraints. The movement direction of the transitioned helix gait on the ground is also the same as that described above.

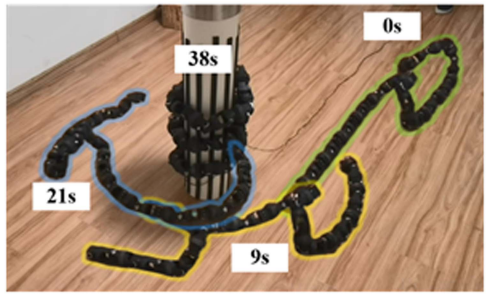

Fig. 14. The transition experiment from crawler gait to helix gait with a cylinder.

In the gait transition with phase control, we use PVC pipe with a diameter of 200 mm as the climbing object. We also attached foam to the vertical direction of the pipe, hoping to increase the friction and reduce the tangential movement of helix. Under the phase control, the arc rolling motion has high robustness to the capture of the cylinder, so the position at which the robot starts the transition in the actual operation does not need to be very accurate. The experimental results are shown in Fig. 14.

The transition action of the robot is controlled by the operator in real time. First, walk straight through the crawler gait, and then select the appropriate turning point to start turning. When the distance from the cylinder is appropriate, the tail begins to transition, and the cylinder is captured by arc segment under phase control. After capturing, the snake robot gradually transition to helix gait for winding and climbing.

It should be noted that the front and rear ends of the robot are in different motion modes, and their kinematic are also different. From the video provided, it is easy to find that when the ground constraint plays a major role, the kinematics of the helix segment is unstable, and the motion along the tangential direction occurs. When the cylinder constraint works more, the helix segment gradually becomes stable.

C. Crawler Front-End Deformation

For the front-end deformation control of the crawler gait, we use (14) to control the lifting segment of the joints. Due to the non integrability of (14), we use numerical integration to estimate the corresponding relationship of relevant parameters in advance to meet the non slip condition in both directions. For example, we set the parameters of the original crawler to $R_{\mathrm{C}} = 180\,\mathrm{mm}, d_{\mathrm{C}} = 200\,\mathrm{mm}, \alpha_{\mathrm{C}} = 60^{\circ}$, e in (14) is taken as 1, and the corresponding roll angle is taken as 110°. In the experiment, a certain gradient time is set for deformation. The experimental process is shown in the Fig. 15.

The video file provided in the attachment contains all the experimental processes of this section.

D. Discussion

The experimental results can verify the extension of gait transition network in this letter. A series of configuration design methods and gait transition motions were demonstrated.

The transition from crawler to helix is typical in connecting forms. In the experiment, we noticed that using arc/helix

Fig. 15. Experimental process of transition motion at the front-end of snake robot with crawler gait.

connecting method to compress the linear body can effectively reduce the size span of the overall configuration of the robot. At the same time, if the compression part is regarded as the base, the base can also be flexibly converted from the rolling state (arc/helix) to the propulsion state (c-pedal), which will have important value in future application research. Crawler to cylindrical helix is an attempt to combine shape control and phase control, but the result did not meet expectations. The turning radius of the Crawler gait cannot be reduced to the same radius as the cylinder, which is related to the module length and joint angle range of the robot snake. Skidding is obvious, which requires further study on the kinematics and dynamics of different gait in future work.

Crawler's front-end deformation is the demand generated in our practical application. It can be seen from the experiment that the range of joint angles required is relatively large, which may require the cooperation of structural design. However, only through the adjustment of local configuration, we can realize the crossing of different scenes, which will effectively improve the motion efficiency of crawler gait and expand its application.

V. Conclusion and Future Work

In this letter, we summarize the existing transition relationship for climbing gaits, and call it gait transition network for snake robot. In the network, the nodes represent the gaits, and the edges represent the transition motion between gaits. Then, we design a variety of gait transition methods according to the difference of snake robot gaits and its application, which extend the current gait transition network and greatly improved the motion efficiency of the snake robot in complex environments.

The improvement of gait transition network will greatly reduce the complexity of the global path planning problem of snake robot, which is our main research topic in the future. With the increase of the module number, the limitation of robot's movement in narrow space will also increase. The introduction of reconfigurable system is one of the ways to solve this problem. There are great differences in the performance of different gait under different module numbers, which will inevitably lead to the evolution/degradation of gait transition network, which makes the integration of reconstruction strategy and motion planning become very interesting. On the other hand, it is found from the experiment that the stability of configuration and the controllability of motion direction in the process of transition motion need to be improved.

References

[1] S. Hirose, *Biologically Inspired Robots: Snake-Like Locomotor and Manipulator*. Oxford, U.K.: Oxford Univ. Press, 1987.
[2] M. Tesch et al., "Parameterized and scripted gaits for modular snake robots," *Adv. Robot.*, vol. 23, no. 9, pp. 1131–1158, 2009.
[3] D. Rollinson and H. Choset, "Pipe network locomotion with a snake robot," *J. Field Robot.*, vol. 33, no. 3, pp. 322–336, 2016.
[4] M. Saito, M. Fukaya, and T. Iwasaki, "Serpentine locomotion with robotic snakes," *IEEE Control Syst. Mag.*, vol. 22, no. 1, pp. 64–81, Feb. 2002.
[5] E. Florian, D. Rollinson, and H. Choset, "Simplified motion modeling for snake robots," in *Proc. IEEE Int. Conf. Robot. Automat.*, 2012, pp. 4216–4221.
[6] K. Lipkin et al., "Differentiable and piecewise differentiable gaits for snake robots," in *Proc. IEEE/RSJ Int. Conf. Intell. Robots Syst.*, 2007, pp. 1864–1869.
[7] J. W. Burdick, J. Radford, and G. S. Chirikjian, "A 'sidewinding' locomotion gait for hyper-redundant robots," in *Proc. IEEE Int. Conf. Robot. Automat.*, 1993, pp. 101–106.
[8] T. Takemori, M. Tanaka, and F. Matsuno, "Gait design for a snake robot by connecting curve segments and experimental demonstration," *IEEE Trans. Robot.*, vol. 34, no. 5, pp. 1384–1391, Oct. 2018.
[9] H. Yamada and S. Hirose, "Study on the 3D shape of active cord mechanism," in *Proc. IEEE Int. Conf. Robot. Automat.*, 2006, pp. 2890–2895.
[10] W. Zhen, C. Gong, and H. Choset, "Modeling rolling gaits of a snake robot," in *Proc. IEEE Int. Conf. Robot. Automat.*, 2015, pp. 3741–3746.
[11] C. Gong, M. J. Travers, X. Fu, and H. Choset, "Extended gait equation for sidewinding," in *Proc. IEEE Int. Conf. Robot. Automat.*, 2013, pp. 5162–5167.
[12] M. Inazawa, T. Takemori, M. Tanaka, and F. Matsuno, "Motion design for a snake robot negotiating complicated pipe structures of a constant diameter," in *Proc. IEEE Int. Conf. Robot. Automat.*, 2020, pp. 8073–8079.
[13] T. Wang et al., "Reconstruction of backbone curves for snake robots," *IEEE Robot. Automat. Lett.*, vol. 6, no. 2, pp. 3264–3270, Apr. 2021.
[14] L. Bai et al., "CPG-based gait generation of the curved-leg hexapod robot with smooth gait transition," *Sensors*, vol. 19, no. 17, 2019, Art. no. 3705.
[15] C. Bal, "Neural coupled central pattern generator based smooth gait transition of a biomimetic hexapod robot," *Neurocomputing*, vol. 420, pp. 210–226, 2021.
[16] D. Zhang, Q. Xiao, and Z. Cao, "Gait generation with smooth transition using neural oscillator network based locomotion control for snake-like robot," in *Proc. IEEE Int. Conf. Soft Robot.*, 2019, pp. 206–211.
[17] G. Droge and M. Egerstedt, "Optimal decentralized gait transitions for snake robots," in *Proc. IEEE Int. Conf. Robot. Automat.*, 2012, pp. 317–322.
[18] X. Xiao et al., "Locomotive reduction for snake robots," in *Proc. IEEE Int. Conf. Robot. Automat.*, 2015, pp. 3735–3740.
[19] T. Takemori, M. Tanaka, and F. Matsuno, "Hoop-passing motion for a snake robot to realize motion transition across different environments," *IEEE Trans. Robot.*, vol. 37, no. 5, pp. 1696–1711, Oct. 2021.
[20] D. Rollinson and H. Choset, "Virtual chassis for snake robots," in *Proc. IEEE/RSJ Int. Conf. Intell. Robots Syst.*, 2011, pp. 221–226.
[21] T. Takemori, M. Tanaka, and F. Matsuno, "Ladder climbing with a snake robot," in *Proc. IEEE/RSJ Int. Conf. Intell. Robots Syst.*, 2018, pp. 1–9.
[22] T. Kamegawa, T. Baba, and A. Gofuku, "V-shift control for snake robot moving the inside of a pipe with helical rolling motion," in *Proc. IEEE Int. Symp. Saf., Secur., Rescue Robot.*, 2011, pp. 1–6.
[23] M. Inazawa, T. Takemori, M. Tanaka, and F. Matsuno, "Unified approach to the motion design for a snake robot negotiating complicated pipe structures," *Front. Robot. AI*, vol. 8, 2021, Art. no. 629368.